Angle of Attack and True Airspeed failure sensor detection and recovery based on Unscented Kalman Filters for the ALPHA vehicle

García de Marina, H.*, Marcos, A.*, Haya, R.*

** Deimos Space SLU, Tres Cantos (Madrid), Spain 28760*
e-mail: hgdemarina@gmail.com,{andres.marcos,rodrigo.haya}@deimos-space.com

Abstract: As part of a European Framework project, FAST20XX, well known and advanced fault detection, identification and recovery techniques are evaluated for its use on a future low-energy sub-orbital transportation concept. In this article, an on-board FDIR scheme for faults in the Angle of Attack and True Airspeed sensors is presented. The FDIR logic is based on the Unscented Kalman Filter theory and the resulting design performs on-line sensor evaluation and compensation of the Navigation component of the vehicle's GNC system. A Monte Carlo campaign using a high-fidelity model of the vehicle is used to demonstrate the performance and robustness of the scheme.

Keywords: Fault Detection and Identification, Kalman Filters, Sensor Compensation

1. INTRODUCTION

This paper considers the problem of designing discrete-time Unscented Kalman Filters (UKF) for Failure Detection, Identification and Recovery (FDIR). This type of filters has been widely used in fault detection and health monitoring of dynamic systems Blanke(2003), Chen(1999), Luppold(1989). In the present case, the UKF technique is employed for failure detection and recovery of two coupled sensors, those for the angle of attack and true airspeed, during the re-entry phase of a sub-orbital transport vehicle. The FDIR modele is divided into two distinct stages, each with a single filter: detection and recovery.

Kalman filter FDIR approaches are based on the analysis of the residual signals resulting from the Kalman filter. In essence, when the system operates in a fault-free situation the normalized residual signals from the Kalman filter are Gaussian white noise with zero mean. Faults change the system dynamics by causing surges or drifts of the state vector components, abnormal measurements, sudden shifts in the measurement sensor and other difficulties. For linear dynamic system with white process and measurement noise, the Kalman filter is known to be an optimal estimator. Unfortunately, most real applications are non-linear, and moreover, the noise is not usually Gaussian nor the system model can be accurately modeled.

A sigma-point Kalman Filter based on the unscented transform (UKF) is examined in comparison to the traditional Extender Kalman Filter (EKF) since the latter is in general not an optimal estimator. In addition, if the initial state is wrong or if the process is modelled incorrectly, the EKF may quickly diverge. The UKF on the other hand, uses non-linear models directly (to estimate the covariance matrix of the state vector) and it can be tuned to fit other types of noise besides Gaussian. Therefore, the predictions of a UKF are expected to be more accurate, see reference Julier(1997).

The results presented in this article are part of a European Framework FP7 co-funded project termed "Future High-Altitude High-Speed Transport 20XX" (FAST20XX) Mack(2010). The project, led by the European Space Agency (ESA), involves 17 different partners across Europe and started in December 2009 with a duration of three years. The project aims at exploring the borderline between aviation and space by investigating suborbital vehicles. The main focus is the identification and mastering of critical technologies for such vehicles rather than the vehicle development itself.

The layout of the paper is as follows. The first section of the paper is devoted to the formulation of the problem, including the kinematical model employed and the architecture of the FDIR system. Subsequently, nonlinear simulations of the re-entry phase of the suborbital vehicle are performed in a Monte Carlo setting to fully evaluate the proposed FDIR system. In the final section of the paper, the conclusions are drawn, including some guidelines for future work.

2. PROBLEM FORMULATION

In this section the formulation of the problem is given. This formulation consists of a brief description of: the vehicle, the kinematical model and the FDIR architecture.

The low-energy suborbital transportation vehicle concept (ALPHA) used in FAST20XX is directed towards an airplane-launched aircraft for short-range sub-orbital flights. The configuration, see Fig. 1, will follow, on the one hand, the design of SpaceShip-One because its concept has already been proven, and on the other hand, it will take advantage of the successfully flown German RLV demonstrator Phoenix for which a large aerodynamic database is available. Depending on the vehicle size, the number of passengers can

range from three to five (two to four passengers plus one pilot).

Fig. 1. ALPHA concept (Phoenix vehicle, courtesy EADS)

Although each vehicle has its own characteristics (geometric and aerodynamic coefficients) and therefore its own dynamical model, it is possible to determine the Angle of Attack (α) and the True Air Speed (V_{tas}) from a kinematical perspective making it independent on the vehicle characteristics. In Subsection 2.1, the mathematical formulation of the system is given based on the kinematical relations, while Subsection 2.2 presents the design of the FDIR scheme for this system based on UKF.

2.1 Kinematical equations

Assuming the vehicle is equipped with an Angle of Attack (α), Angle of Sideslip (β) and dynamic pressure sensors, as well as with an Inertial Measurement Unit (IMU) with three-axis accelerometers and three-axis gyroscopes, kinematic relations can be used to determine

Kinematics equations, Stevens (2003), relate the vehicle's relative velocity with respect to the wind [U', V', W'] with the aerodynamic angles α and β, and the True Air Speed V_{tas}:

$$\begin{cases} U' = V_{tas}\cos\alpha\cos\beta \\ V' = V_{tas}\sin\beta \\ W' = V_{tas}\sin\alpha\cos\beta \end{cases} \quad (1)$$

Using the above equation, it is simple to deduce the derivative with respect to time for α, β and V_{tas}:

$$\dot{\alpha} = \frac{\dot{W}'\cos\alpha - \dot{U}'\sin\alpha}{V_{tas}\cos\beta} \quad (2)$$

$$\dot{\beta} = \frac{\dot{V}' - \dot{V}_{tas}\sin\beta}{V_{tas}\cos\beta} \quad (3)$$

$$\dot{V}_{tas} = \dot{U}'\cos\alpha\cos\beta + \dot{V}'\sin\beta + \dot{W}'\sin\alpha\cos\beta \quad (4)$$

Where $\dot{U}', \dot{V}'$ and $\dot{W}'$ are the vehicle's relative velocity with respect to the wind derivatives.

2.2 FDIR system

Two discrete UKF filters are used, the first one detects faults in the α or V_{tas} sensors in α or V_{tas} sensors while the second UKF filter is used to compensate α sensor malfunctions. Both filters are fed by the Sensors and Navigation component of the vehicle's GNC. In order to distinguish between both filters, the subscripts FD ("Fault Detection") and FC ("fault compensation") are used. **Fig. 2** shows the FDI system proposed.

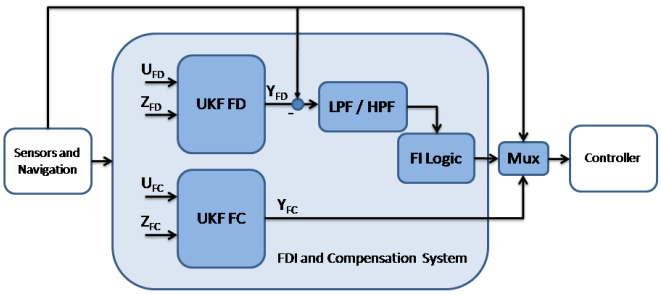

Fig. 2 FDIR System architecture, where LPF and HPF are Low and High pass filters respectively.

The Failure Detection is carried out in two steps, Zolghadri(1998): residual generation and residual evaluation. First, a residual is generated by the UKF_{FD}. Then, the residual is filtered and a logic algorithm is applied to determine whether a failure is present or not.

The Failure Compensation is carried out in only one step by estimating the biases produced by the failures to compensate the Angle of Attack reading, which feeds into the controller.

2.3 The Fault Detection filter

The UKF_{FD} is a tracking filter with the following state vector:

$$x_{FD}(k) = \begin{bmatrix} V_{tas}(k) & \alpha(k) \end{bmatrix}^T \quad (5)$$

The UKF_{FD} employs as the system model a discrete version of (2) and (4) with the following assumptions and simplifications:

- The vehicle's relative velocity with respect to the wind derivative [$\dot{U}', \dot{V}', \dot{W}'$] is equal to the inertial velocity derivatives in body frame [$\dot{U}, \dot{V}, \dot{W}$].
- Sideslip is assumed to be zero.

The first assumption implies considering the wind vector as locally constant, while the second assumption allows discarding β as an input to the filter. With these assumptions, the UKF_{FD} system model is:

$$V_{tas}(k+1) = V_{tas}(k) + \left(\dot{U}(k)\cos\alpha(k) + \dot{W}(k)\sin\alpha(k)\right)\Delta T \quad (6)$$

$$\alpha(k+1) = \alpha(k) + \left(\frac{\dot{W}(k)\cos\alpha(k) - \dot{U}(k)\sin\alpha(k)}{V_{tas}(k)}\right)\Delta T \quad (7)$$

The integration method chosen is Euler and ΔT is the filter's sample time.

Both (the FD and FT) UKF filters are fed by the on-board Sensors and Navigation System. The inertial velocity derivatives in body frame $[\dot{U}(k),\dot{V}(k),\dot{W}(k)]$ are provided by the IMU. Indeed, the IMU is assumed to provide inertial velocity sums in both, the body and the navigation frames. The IMU also provides the attitude between these two frames in quaternion form. The Navigation system uses these inputs to estimate the position, velocity and acceleration in the navigation frame. This acceleration is compensated with the gravity vector (based on a J2 model) and the centripetal and Coriolis accelerations.

The compensated acceleration vector serves as input to the U_{FD} in **Fig. 2**. The observation model of the UKF_{FD} is a 2x2 identity matrix, which means that the observation is directly compared with the V_{tas} and α measurements from the on-board sensors (Z_{FD} in **Fig. 2**). The UKF_{FD} output Y_{FD} is its state vector. This signal contains the information to detect a potential fault. The treatment of this primary residual signal is further discussed in the Simulation Results Section.

2.4 The Fault Compensator filter

The UKF_{FC} is a bias estimation filter with the following state vector:

$$x_{FC}(k) = \begin{bmatrix} V_{tas}(k) & b_\alpha(k) & \beta(k) \end{bmatrix}^T \tag{8}$$

Where $b_\alpha(k)$ is an estimated bias in the α sensor.

The UKF_{FC} includes in its system model the discrete versions of (3) and (4) using the first assumption from before but not assuming β equal to zero but practically at a small value throughout the mission. Thus, the trigonometric functions involving β can be written in their small angle approximation form while taking into account the more realistic scenario – typically, re-entry vehicles try to minimize sideslip.

Therefore the UKF_{FC} system model is:

$$\begin{aligned} V_{tas}(k+1) &= V_{tas}(k) + \dot{U}(k)\cos\big(\alpha(k) - b_\alpha(k)\big)\Delta T \\ &+ \dot{W}(k)\sin\big(\alpha(k) - b_\alpha(k)\big)\Delta T + \dot{V}(k)\beta)\Delta T \end{aligned} \tag{9}$$

$$\beta(k+1) = \beta(k) + \left(\frac{\dot{V}(k) - \beta(k)\dot{V}_{tas}(k)}{V_{tas}(k)}\right)\Delta T \tag{10}$$

$$b_\alpha(k+1) = b_\alpha(k) \tag{11}$$

Where $\dot{V}_{tas}(k)$ in (10) is the third term of (9) divided by ΔT, the filter's sample time.

As mentioned before, $[\dot{U}(k),\dot{V}(k),\dot{W}(k)]$ is provided by the Navigation system so that the input set for U_{FC} (see **Fig. 2**) is completed with $\alpha(k)$ which is provided by the α sensor.

The estimated bias b_α is modelled as a constant over time. The convergence time of this variable to its true value depends on the ratio of the sample time and the true first derivative of b_α mostly, but also on the process noise covariance associate to it –the lower its value, the slower the convergence time albeit more accurate Efimov(2010).

The observation model of UKF_{FC} is then given by:

$$H_{FC} = \begin{pmatrix} 1 & 0 & 0 \\ 0 & 0 & 1 \end{pmatrix} \tag{12}$$

This observation models means that the filter output is directly compared to the V_{tas} and β sensors (Z_{FC} in **Fig. 2**). The output Y_{FC} is formed by the estimated bias in the α sensor and the β estimation. The former is used to compensate the α measurement once the fault isolation (FI) logic declares a failure in the sensor, while the latter estimation could be employed in the Navigation system if no failures are detected/declared.

3. SIMULATION ENVIRONMENT AND REFERENCE SCENARIO

3.1 Simulation Environment

The Functional Engineering Simulator (FES) for the ALPHA vehicle, ALPHA-FES, is Deimos' reference simulator within the FAST20XX project. The goal of the ALPHA-FES tool is to provide a simulation platform able to reproduce the dynamics and environment of the ALPHA vehicle in both ascent and re-entry scenario.

Detailed models of the vehicle, avionics and GNC components are plugged and simulated with respect to the selected scenario and the simulator user needs. System components configuration, raw data saving and Monte Carlo functionalities are internally provided by the simulator and can be easily managed by the system user through the simulator database. Post-processing functions for the computation and the plot of interesting profiles are provided.

All the simulations presented in this chapter have the following common features:

- 6 Degrees of Freedom nonlinear ALPHA dynamics.
- A nonlinear dynamic inversion (NDI) inner-loop controller –similar to that in Marcos (2007)
- The 1962 USA atmospheric model
- Realistic sensor noise for the control measurements
- Ellipsoid planet shape
- Aerodynamic actuators are magnitude/ rate saturated while RCS are magnitude saturated
- Parametric uncertainty for mass, moment of inertia, center of gravity and aerodynamic coefficients (independent of the estimated coefficients used by the NDI controller)

3.2 FDIR Scenario and fault selection

In the present FDIR scenario, a focused time period of the re-entry phase is considered. This is the period during the re-entry phase covering from 180 to 500 seconds. This focused period of the trajectory was chosen for the FDIR design as it corresponds to a period where full aerodynamic controls are employed and where the vehicle response changes sufficiently to test the robustness properties of the design filters over a sufficient large time period.

The specific problem undertaken is to design an FDIR system that can be retrofitted to the existing closed-loop system comprised by the nonlinear vehicle model and the NDI controller. As previously shown, the FDIR system is able to detect faults in the α and V_{tas} sensors, which are critical parameters for the controller. Note that only independent fault cases are considered.

The first fault scenario is a combination of bias and drift faults, first for the α sensor followed by similar fault combination for the V_{tas} sensor. The α bias fault starts at 220 seconds with a drift of 0.3 deg/s until it reaches the maximum simulated bias fault amplitude at 230 seconds. This bias fault value is held constant until 240 seconds, after which the fault drifts back to 0 degrees at a rate of -0.3 deg/s, with the fault ending at 250 seconds. The V_{tas} fault start at 280 seconds, with a drift of 0.3m/s that reaches the maximum bias fault amplitude at 290 seconds. The bias fault value is held constant until 300 seconds, after which the fault drifts back to zero at a rate of -0.3m/s, with the fault ending at 310 seconds.

Fig.3 shows the effect of this fault in the closed-loop. The controller receives the estimated α (blue dotted) as input and it believes is tracking correctly the reference value (black solid) from the guidance system. However, the fault introduced leads a divergence with respect to the reference value which is reflected by the true "flown" value (red dashed).

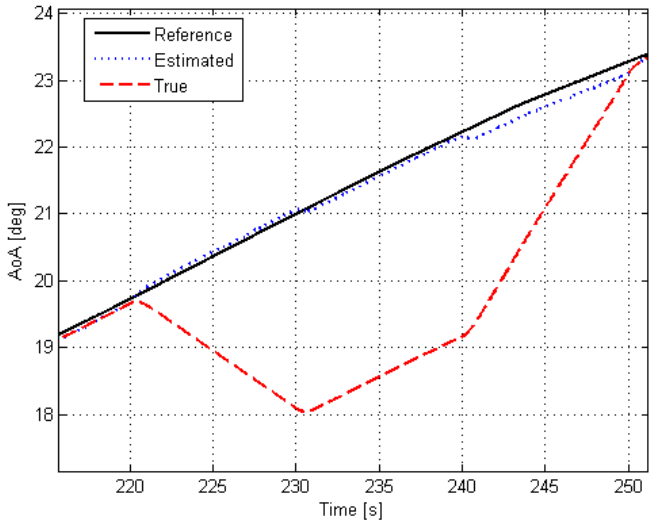

Fig. 3 Evolution of the Angle of Attack in the fault scenario without any compensation

4. SIMULATION ANALYSIS AND RESULTS

This section describes the analysis of the FDIR system within the closed-loop and its derived results. A Monte Carlo analysis of 1000 runs of the FDIR system was performed to assure the stability of the system throughout the re-entry phase.

Fig. 4 shows, in the first and third graph, the α and V_{tas} residual signals from the UKF_{FD} while the second and fourth graphs correspond to their filtered versions. We are interested in changes in the monotony of these signals. In the case of the α signal, a simple low pass filter is enough to capture the failure drifts (second graph). For V_{tas} due to the simplifications adopted, the estimation does not converge to zero in the UKF_{FD}. This non-zero convergence really is not important as this filter is only for detecting failures. A high pass filter can capture the failure drifts (fourth graph), which have the same shape as the α drifts. Observe that the V_{tas} filtered residual signal is coupled with that for the α signal (e.g. the "false detection" in the region 200-250 seconds) but not vice versa. Therefore, it is straight forward to use some logic to distinguish between an α or V_{tas} failure.

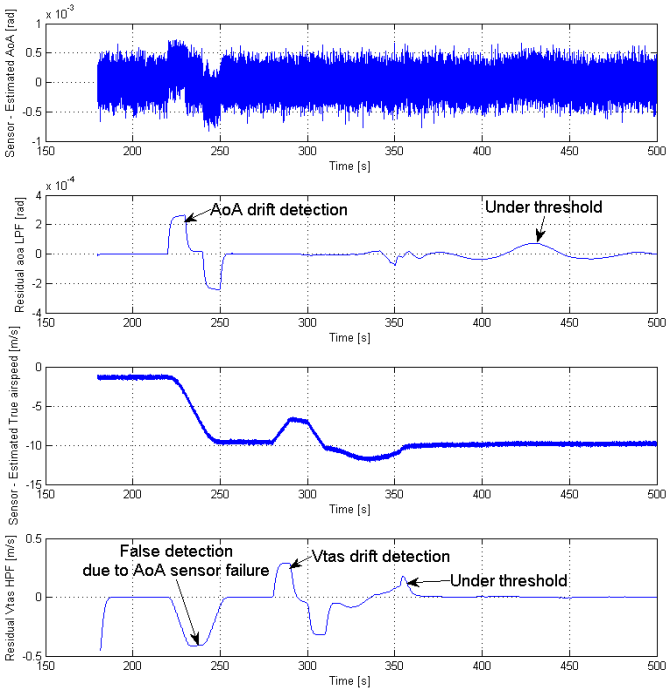

Fig. 4 Raw residual Angle of Attack and Vtas signals before and after a low pass filter and high pass filter respectively

Fig.5 shows in detail the α filtered residual signal (top graph of Fig.4) for the period in which the fault is active. It is observed that when the drift fault is triggered, the residual signal starts to grow in absolute value (regions 220-225 and 240-245 seconds), and when the bias is constant, the residual signal converges to a non-zero value (region 230-240 seconds).

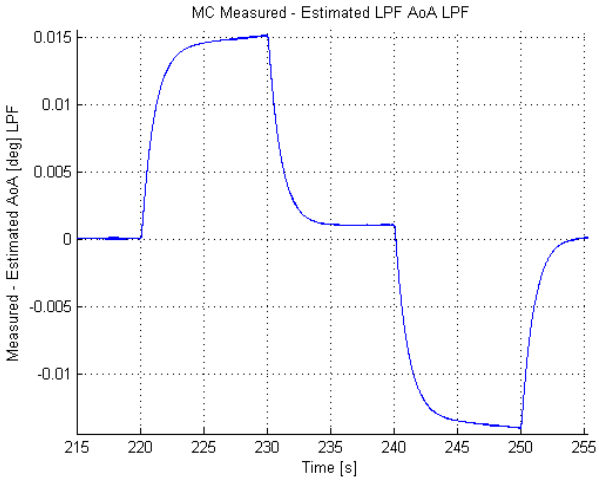

Fig. 5 Low-pass filter residual α signal.

The logic used to distinguish between an α or V_{tas} sensor fault is based on a Schmitt trigger. As the V_{tas} residual signal is coupled with α faults but not vice cersa, if an α failure is detected then the V_{tas} failure is ignored. The thresholds are selected according to the filtered residual signals shown in Fig.4. It can be observed in the α low-pass filtered residual of Fig.4 that the signal is clearly different to zero at 350 second. This behaviour is due to the simplified system model used and to the errors in the accelerations (which are inputs to the UKF_{FD} from the Navigation system). In Fig.6 these effects are clearly observed in the 220-250 seconds region (where the α estimate is affected by the drift and bias) and around the 350 seconds (where the α estimated is corrupted by model and input errors to the tracking filter UKF_{FD}).

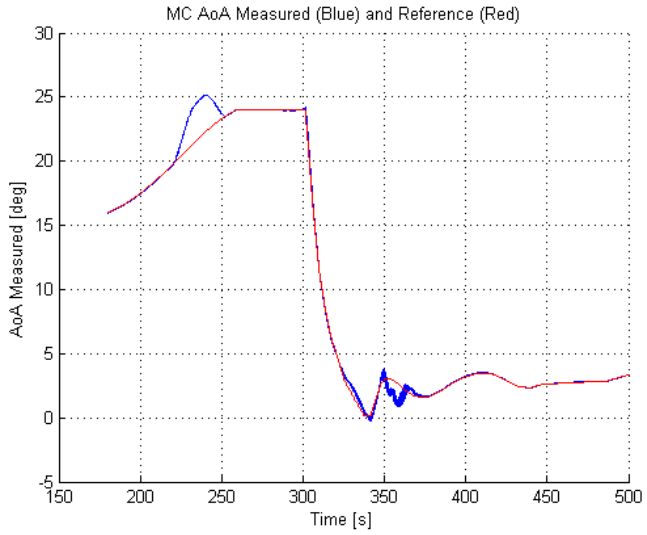

Fig. 6 Angle of attack measured without compensation vs Angle of attack reference.

A set of 100 random free fault are used to set the threshold values for the FDIR logic over the absolute maximum value in the worst-case condition, in order to avoid false alarms. Once a fault drift starts, the Schmitt trigger can be modified to expect the bias being held and/or the drift to be cancelled such as in Fig.5.

Fig.7 shows the health monitoring flag for the α and V_{tas} sensor failures based on the previous logic. Note that when an α flag is triggered, the V_{tas} residual signal is ignored, therefore the FDIR logic correctly distinguishes between the two possible failures.

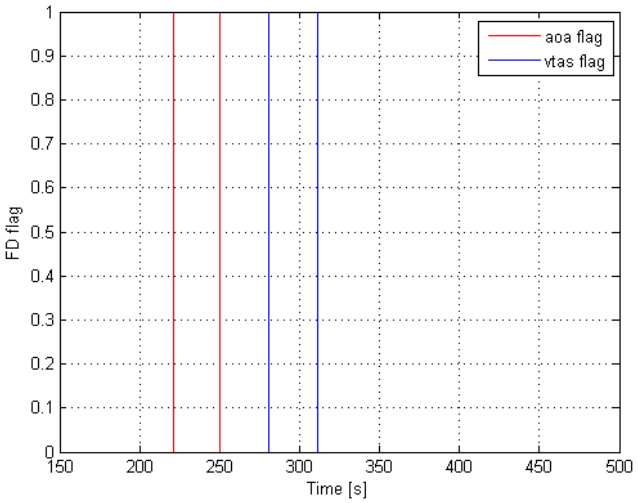

Fig. 7 Angle of attack and V_{tas} failure flags.

Monte Carlo assessment showed that the true detection ratio is 100% with a mean detection time of 0.49 seconds for both sensors. Once the failure disappears, the mean detection time (to re-capture the true value) is 1.03 seconds for both sensors. Both times heavily depends on the chosen threshold, with a conservative threshold implying a slower detection.

Fig. 8 shows the estimated bias for the angle of attack sensor, which is one of the UKF_{FC} outputs. It clearly estimates the drift and bias during the failure period. Biases estimated out of the failure period are due to the approximation model and input errors from the Navigation module and/or due to the V_{tas} sensor fault.

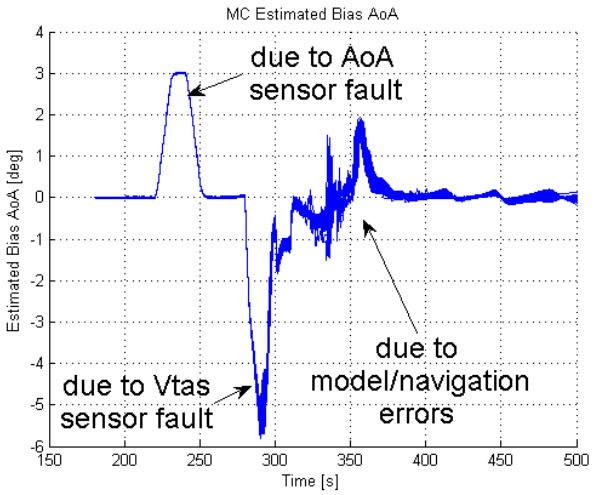

Fig. 8 Estimation of the bias of the Angle of Attack.

Note that the fault compensation, shown in Fig.9, only occurs when the α flag is activated by the health management system so that the latter bias are not affecting the system. Fig.10 shows the total error average in the Monte Carlo campaign

between the true and compensated angle of attacks. Note that with the compensation in α, the error is less than 0.5 degrees.

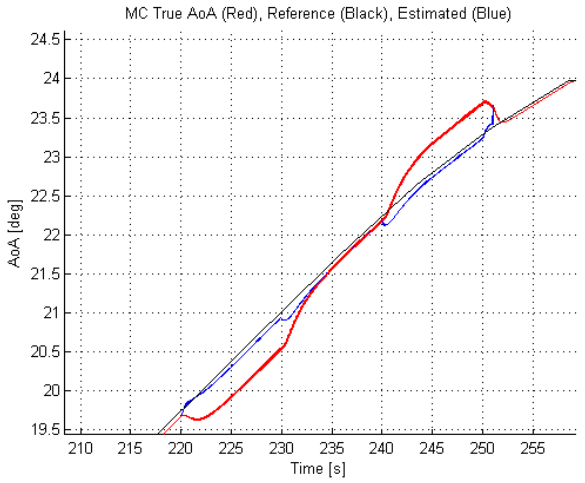

Fig. 9 True (Red), Estimated (Blue) and Reference (Black) Angle of Attack during the failure period.

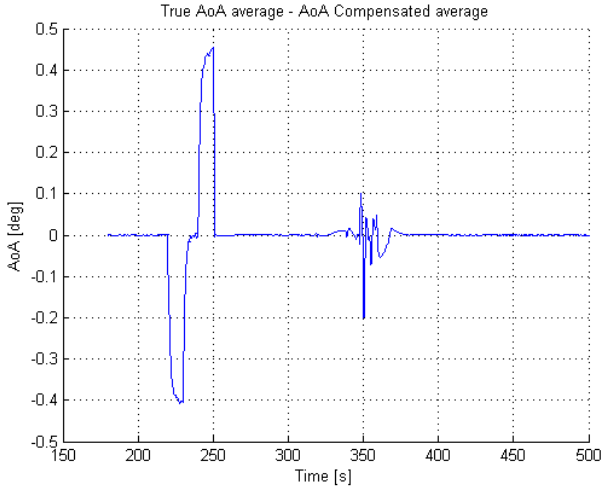

Fig. 10 Error between True and Compensated averages of Angle of Attacks.

Finally, as an additional advantage of the proposed filter, Fig.11 shows the angle of sideslip estimated by the UKF_{FD} (blue solid line), which clearly results in a cleaner signal than the direct sensor reading (black solid line).

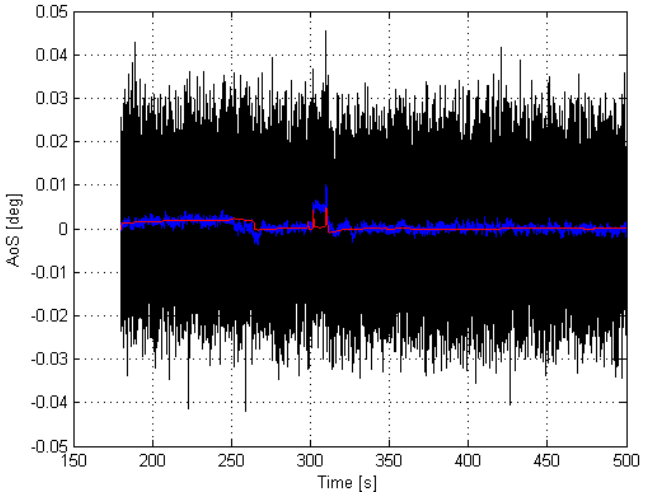

Fig. 11 Angle of sideslip estimation.

5. CONCLUSIONS AND FUTHER WORK

In this paper a method for failure detection in the Angle Of Attack and True Airspeed sensors, and recovery of the Angle Of Attack failure has been introduced. The method is based on tracking and estimator UKF filters and has assessed using a Monte Carlo campaign of the re-entry nonlinear simulator.

Simulations show that the drift failure is correctly identified by the filtered residual signal, and therefore can be used for compensation of this kind of failure without an extra estimator filter.

6. ACKNOWLEDGMENT

This work was performed within the “Future High-Altitude High-Speed Transport 20XX” (FAST20XX) coordinated by ESA-ESTEC, and supported by the EU within the 7th Framework Programme Theme Transport, Contract no.: ACP8-GA-2009-233816. Further info on FAST20XX can be found on http://www.esa.int/fast20xx.

The work was performed while the first author was working at Deimos Space SLU. From February 2012 he is a PhD candidate at the University of Groningen.

REFERENCES

Blanke M., Kinnaert M., Lunze M., et Staroswiecki M. (2003). *Diagnosis and fault tolerant control*, Springer, New York.

Chen J., Patton R.J.(1999). *Robust Model-Based Fault Diagnosis for Dynamic Systems*. Kluwer Academic Publishers, Norwell, MA.

Efimov D., Zolghadri A., Simon P. (2010). Improving fault detection abilities of extended Kalman filters by covariance matrices adjustment. *Coference on Control and Fault Tolerant Systems*. France.

Julier S.J., Uhlmann J.K. (1997). A new extension of the Kalman Filter to non-linear systems. *Proc. Int. Symp. Aerospace/Defense Sensing, Simulation and Control*. Orlando, FL, pp 182--193.

Luppold R.H., Roman J.R., Gallops G.W., Kerr L J.(1989) Estimating in-Flight Performance Variations Using Kalman Filter Concepts. *AIAA/SAE/ASME/ASEE 25th Joint Propulsion Conference*. Montery, CA.

Mack, A., Steelant, J., Kordulla, W., (2010) “FAST20XX: Future High-Altitude High-Speed Transport for the Next Decades,” SpacePropulsion 2010, San Sebastian, Spain.

Marcos, A., Peñín, L.F., Caramagno, A., Sommer, J., Belau, W., (2007) Atmospheric Re-Entry NDI Control Design for the Hopper RLV Concept, 17th IFAC Symposium on Automatic Control in Aerospace, Toulouse

Stevens B.L., Lewis F.L. (2003). *Aircraft Control and Simulation*. John Viely and sons.

Zolghadri A., Goetz C., Bergeon B., Denoise X (1998). Integrity monitoring of flight parameters using analytical redundancy. *Proc. UKACC internation coference on control (CONTROL ’98)*. UK, pp 1534—1539.